Insight into the Mechanism of Inactivation of Ribonucleotide Reductase by Gemcitabine 5′-Diphosphate in the Presence or Absence of Reductant[†]

Erin Artin,[‡,||] Jun Wang,[‡] Gregory J. S. Lohman,[‡] Kenichi Yokoyama,[‡] Guixue Yu,[‡] Robert G. Griffin,[‡] Galit Bar,[‡] and JoAnne Stubbe*[,‡,§]

[‡]*Departments of Chemistry and* [§]*Biology, Massachusetts Institute of Technology, Cambridge, Massachusetts 02139*
[||]*Present address: Intelligent BioSystems, 34 Bear Hill Road, Waltham, MA 02451*

ABSTRACT: Gemcitabine 5′-diphosphate (F_2CDP) is a potent inhibitor of ribonucleotide reductases (RNRs), enzymes that convert nucleotides (NDPs) to deoxynucleotides and are essential for DNA replication and repair. The *Escherichia coli* RNR, an $\alpha2\beta2$ complex, when incubated with 1 equiv of F_2CDP catalyzes the release of two fluorides and cytosine concomitant with enzyme inactivation. In the presence of reductant (thioredoxin/thioredoxin reductase/NADPH or DTT), the enzyme inactivation results from its covalent labeling of α with the sugar of F_2CDP (one label/$\alpha2\beta2$). SDS-PAGE analysis of the inactivated RNR without boiling of the sample reveals that α migrates as an 87 and 110 kDa protein in a ratio of 0.6:0.4. When the reductant is omitted, RNR is inactivated by loss of the essential tyrosyl radical and formation of a new radical. Inactivation studies with C225S-α in the presence or absence of reductants, reveal it behaves like wt-RNR in the absence of reductant. Inactivated C225S-α migrates as an 87 kDa protein and is not covalently modified. C225 is one of the cysteines in RNR's active site that supplies reducing equivalents to make dNDPs. To identify the new radical formed, $[1'-^2H]-F_2CDP$ was studied with wt- and C225S-RNR by 9 and 140 GHz EPR spectroscopy. These studies revealed that the new radical is a nucleotide derived with g values of g_x 2.00738, g_y 2.00592, and g_z 2.00230 and with altered hyperfine interactions (apparent triplet collapsed to a doublet) relative to $[1'-^1H]-F_2CDP$. The EPR features are very similar to those we recently reported for the nucleotide radical generated with CDP and E441Q-RNR.

2′,2′-Difluorodeoxycytidine (F_2C or gemcitabine)[1] is used clinically in the treatment of nonsmall cell lung and pancreatic cancers (1−5). Its biological activity results from its inhibitory action on multiple steps required for DNA biosynthesis. F_2C is transported into the cell via three nucleoside transporters (ENT1, ENT2, and CNT1). It is then phosphorylated by human deoxycytidine kinase (hdCK) to the 5′-monophosphate (F_2CMP) and to the diphosphate (F_2CDP) by human UMP/CMP kinase (hCMPK) (6−8). Conversion to the triphosphate (F_2CTP) is most likely carried out by nucleoside diphosphate kinases (9). F_2CTP is believed to be the major cause of apoptosis in treated malignant cells, exerting its effect by its incorporation into DNA where it causes stalling of DNA synthesis and DNA chain termination (2). This mode of action is potentiated by the ability of F_2CDP to inhibit human ribonucleotide reductase (hRNR), the enzyme responsible for the conversion of nucleoside diphosphates to deoxynucleoside diphosphates (dNDPs) (10, 11). This inhibition depletes levels of all dNDPs, and consequently dNTPs, in the cell and enhances the ability of F_2CTP to compete with dCTP for incorporation into DNA (12, 13). Furthermore, depletion of dCTP releases the tight feedback inhibition of hdCK by dCTP and results in elevated levels of F_2CDP and F_2CTP (14). The ability of F_2C to affect its own metabolism is likely responsible for its unique cytotoxic properties relative to other nucleosides. The detailed understanding of the mechanism of inhibition of RNR by F_2CDP and the mechanism(s) for resistance to F_2C by overexpression of each of the subunits of RNR, α or β, associated with different cancers are active areas to research (4, 5). This paper reports new insight into the mechanism of inhibition of *Escherichia coli* RNR, a model for the hRNR, under conditions in which reductant is absent. A model for the inactivation process that accommodates available data is proposed.

Inhibition of RNR by nucleotides of F_2C has been most extensively studied with enzymes from *E. coli* and *Lactobacillus leichmannii* (15−17). The *E. coli* RNR is composed of two subunits, α and β. The active site for nucleotide reduction is in $\alpha2$, which is structurally homologous to the α of the *L. leichmannii* RNR, which is a monomer. The $\beta2$ subunit of *E. coli* RNR houses the diferric-tyrosyl radical ($Y\cdot$) which initiates nucleotide reduction on α, while adenosylcobalamin initiates nucleotide reduction in the *L. leichmannii* RNR. The studies on the *E. coli* RNR revealed that the mechanism of inhibition by

---

*To whom correspondence should be addressed. Tel: (617) 253-1814. Fax: (617) 258-7247. E-mail: stubbe@mit.edu.

[1]Abbreviations: RNR, ribonucleotide reductase; α, ribonucleotide reductase large subunit; β, ribonucleotide reductase small subunit; hRNR, human RNR; dNDP, deoxynucleoside 5′-diphosphate; NDP, nucleoside 5′-diphosphate; equiv, equivalents; β-ME, β-mercaptoethanol; TR, thioredoxin; TRR, thioredoxin reductase; SA, specific activity; wt, wild type; TEAB, triethylammonium bicarbonate; hdCK, human deoxycytidine kinase; hCMPK, human UMP/CMP kinase; $Y\cdot$, tyrosyl radical; GST-CMK, glutathione *S*-transferase fusion to human UMP/CMP kinase; F_2C, 2′,2′-dideoxydifluorocytidine or gemcitabine; F_2CDP, 5′-diphosphate of F_2C; F_2CTP, 5′-triphosphate of F_2C; buffer A, 50 mM HEPES, pH 7.6, 15 mM $MgSO_4$, and 1 mM EDTA.

F_2CDP is reductant-dependent (*15*). In the presence of a reducing system, thioredoxin/thioredoxin reductase/NADPH (TR/TRR/NADPH) or 1,4-dithiothreitol (DTT), inhibition resulted predominantly from covalent labeling of α (one label/α2) (*18*). This labeling was accompanied by increased interaction between the two subunits, such that they migrated as an α2β2 complex by size exclusion chromatography. In the absence of reductant, inhibition resulted predominantly from the loss of the essential Y· located on β2. The Y· loss was accompanied by formation of a "new" stable radical (*15*). The structure of the new radical, which displays a triplet EPR line shape at 9 GHz, was proposed to arise from interactions with two $I = \frac{1}{2}$ nuclei. However, EPR spectra recorded in ^2H_2O and with uniformly deuterated α revealed no changes in the hyperfine interactions of the new radical. In addition, initial quantitative analysis of two products accompanying RNR inactivation in the presence and in the absence of reductant suggested that 2 equiv of fluoride and 1 equiv of cytosine per α2β2 were generated. No mechanistic models for inactivation were proposed at that time. More recently, theoretical studies of Ramos and co-workers have resulted in proposed mechanisms for inactivation in the presence and absence of reductant (*19*, *20*).

Our initial studies were carried out with *E. coli* RNR (15 μM) and unlabeled F_2CDP. Using methods we have recently developed to incorporate labels into F_2CDP (^3H and ^2H at C1′, ^3H at C5, and ^2H at C3′), we now report inactivation studies in the presence and absence of reductants with 3 μM wt- and C225S-RNR. C225 is one of the five essential cysteines in α, and its function is to supply the reducing equivalents to make dNDPs concomitant with its oxidation to a disulfide with C462 (*21*, *22*). We show that under physiological conditions, that is, with reducing equivalents available, covalent modification of α2 requires C225. C225S-RNR and F_2CDP in the presence or absence of reductant act like wt-RNR in the absence of reductant. The new radical generated by both wt- and C225S-RNR under these conditions is shown to be nucleotide based, as its production with [1′-^2H]-F_2CDP results in collapse of the 9 GHz triplet hyperfine pattern to a doublet. EPR spectra of the radical at 140 GHz have provided the *g*-values of the new species. The radical produced has properties very similar to the radical generated when E441Q-RNR is reacted with CDP and whose structure was recently established through isotopic labeling, ENDOR and EPR spectroscopy, and computational methods (*23*). A mechanism for the inactivation of RNR by F_2CDP in the absence of reductants and its relationship to inactivation in the presence of reductants is proposed.

MATERIALS AND METHODS

Triethylamine (99% pure) was purchased from Acros and DTT from Mallinckrodt. [5-^3H]-F_2C (1 mCi, 14 Ci/mmol) was purchased from Moravek Biochemicals. All other materials were purchased from Sigma. F_2C was a gift from Eli Lilly and Co. [1′-^2H]-F_2C and [1′-^3H]-F_2CDP (specific activity (SA), 8261 cpm/nmol) were prepared as recently described (*24*, *25*). *E. coli* wt-α2 was purified as described and had a SA of 1800−3000 nmol mg^{-1} min^{-1}. The concentration of α2 (dimer) was determined using ε (280 nm) = 189 mM^{-1} cm^{-1}. α2 was prereduced as previously described (*26*). *E. coli* wt-β2 and 6 × His-β2 (*27*) were isolated as described and had a SA of 6000−7000 nmol mg^{-1} min^{-1}. The concentration of β2 (dimer) was determined using ε (280 nm) = 130.5 mM^{-1} cm^{-1}. The Y· content (1.1−1.2 Y·/β2) was measured by the drop-line correction method and by

EPR spectroscopy (*28*). *E. coli* thioredoxin (TR) was isolated from strain pTrx BL21(DE3) and had a SA of 40 units/mg (*29*). *E. coli* thioredoxin reductase (TRR) was isolated from strain pMR14 K91 and had a SA of 1600 units/mg (*30*). *E. coli* C225S-α2 was purified as previously described (*22*). The clone for hdCK was a gift of Dr. Staffan Eriksson (The Biomedical Center, Uppsala, Sweden) (*31*), and that for the glutathione *S*-transferase fusion with human UMP/CMP kinase (hGST-CMPK) was a gift from Dr. Anna Karlsson (Huddinge University Hospital, Stockholm, Sweden) (*8*).

Time-Dependent Inactivation of α2 and β2 by F_2CDP in the Presence or Absence of Reductants. In a final volume of 110 μL, a typical inactivation mixture contained 1.6 mM ATP, 3 μM prereduced α2 (wt or mutant), 3 μM β2, 3, 6, or 15 μM F_2CDP, and no reductants, or reductants (5 mM DTT or 20 μM TR, 0.5 μM TRR, 1.0 mM NADPH) in 50 mM HEPES, pH 7.6, 15 mM MgSO$_4$, and 1 mM EDTA (buffer A). All reactions were carried out at 25 °C. Inhibition was initiated by the addition of F_2CDP, and an aliquot of the reaction mixture was assayed before addition of F_2CDP for the zero time point. The assay was carried out by two methods. In method 1, a 5 μL aliquot was diluted 10-fold into buffer A to give final concentrations of 1.6 mM ATP, 0.3 μM α2, 0.3 μM β2, 1 mM CDP (or [^3H]-CDP, SA 4000 cpm/nmol), 20 μM TR, 0.5 μM TRR, and 0.2 mM NADPH. In method 2, a 5 μL aliquot was diluted 20-fold into 95 μL of buffer A with a 5-fold excess of a second subunit to give final concentrations of 1.6 mM ATP, 0.15 μM α2 (β2), 0.75 μM β2 (α2), 1 mM CDP (or [^{14}C]-CDP, SA 3200−5000 cpm/nmol), 20 μM TR, 0.5 μM TRR, and 0.2 mM NADPH (1 mM NADPH for the radioactive assay). Deoxynucleotide production was monitored using either the spectrophotometric assay or the radioactive assay with analysis by the method of Steeper and Steuart (*32*).

Phosphorylation of [5-^3H]-F_2C To Form [5-^3H]-F_2CMP. In a final volume of 5 mL, the reaction contained 1 mM [5-^3H]-F_2C (SA of 23000 cpm/nmol), 1.33 mg/mL 6 × His-hdCK (SA 170 nmol mg^{-1} min^{-1}), 2 mM ATP, 2 mM DTT, and 0.5 mg/mL BSA in 50 mM Tris (pH 7.6), 100 mM KCl, and 5 mM MgCl$_2$. The reaction was initiated by the addition of enzyme and incubated at 37 °C for 10 min. Anion-exchange purification of the monophosphate was carried out on a 15 mL DEAE A-25 Sephadex column (1 × 19 cm) with a 90 × 90 mL linear gradient from 0.005 to 0.4 M triethylammonium bicarbonate (TEAB), pH 7.5. Fractions of 9 mL were collected. Five microliters of each fraction was analyzed for radioactivity in 10 mL of Emulsifier-Safe scintillation fluid (Packard) using a Beckman LS 6500 scintillation counter. Fractions 18−24 were pooled, and excess TEAB was removed in vacuo. The product was obtained in 93% yield quantitated by UV−vis absorption (λ_{max} 271 nm, λ_{min} 249 nm).

Phosphorylation of [5-^3H]-F_2CMP to [5-^3H]-F_2CDP. The reaction contained the following in a final volume of 4.65 mL: 1 mM [5-^3H]-F_2CMP, 65 μg/mL hGST-CMPK (SA 4.8 μmol mg^{-1} min^{-1}), 4 mM ATP, and 2 mM DTT in 50 mM Tris (pH 8.0) and 5 mM MgCl$_2$. Reactions were initiated by addition of enzyme and incubated at 37 °C for 30 min. The diphosphate was purified by DEAE-Sephadex A-25 chromatography (15 mL, 1 × 19 cm) using a 120 × 120 mL linear gradient of 5 mM to 0.6 M TEAB (pH 7.5). Fractions (6 mL) were collected and assayed by scintillation counting. Fractions 28−36 were pooled, and the TEAB was removed in vacuo. F_2CDP and ADP coeluted, and the ADP was removed subsequent to periodate

oxidation. Sodium periodate (0.5 M) was added to a final concentration of 18.6 mM (4 equiv relative to starting [5-^{3}H]-F$_2$CMP). The mixture was incubated at 37 °C for 10 min, and then 4 M methylamine was added to a final concentration of 100 mM and the mixture incubated at 37 °C for 20 min. The 4 M methylamine stock solution was freshly prepared from a 40% aqueous solution (Aldrich), and the pH was adjusted to 7.3 by the dropwise addition of 85% phosphoric acid with stirring on ice. The oxidative cleavage was quenched by the addition of L-rhamnose to a final concentration of 37.5 mM (8 equiv relative to starting [5-^{3}H]-F$_2$CMP) followed by incubation at 37 °C for 10 min. To remove the pyrophosphate generated during this process, the reaction was brought to 33 mM Tris (pH 7.2) by addition of 0.33 volume of 100 mM Tris (pH 7.2) and incubated with 5 units/1.5 mL inorganic pyrophosphatase from baker's yeast (E.C. 3.6.1.1; Sigma) in the presence of 1.6 mM MgCl$_2$ at 25 °C for 30 min. [5-^{3}H]-F$_2$CDP was purified on a 15 mL DEAE-Sephadex A-25 column (1 × 19 cm) using a 120 × 120 mL linear gradient of 0.005 to 0.6 M TEAB (pH 7.5). Fractions (6 mL) were collected and assayed by scintillation counting. Fractions 28−36 at 0.4 M TEAB were pooled and concentrated in vacuo to give 78% yield by UV absorption. ^{1}H NMR was acquired on a 500 MHz INOVA spectrometer from Varian. The spectrum was referenced to H$_2$O: NMR (D$_2$O, pH 5.6) δ 4.13 (m, 1H), 4.30 (m, 2H), 4.56 (m, 1H), 6.10 (d, J = 7.6 Hz, 1H), 6.20 (t, J = 7.0 Hz, 1H), 7.85 (d, J = 7.6 Hz, 1H). The ^{31}P NMR was acquired on a 300 MHz MERCURY spectrometer from Varian using 85% H$_3$PO$_4$ in water as the external standard: ^{31}P NMR (D$_2$O, pH 5.6) δ −10.08 (d, J = 20.4 Hz, 1P), −5.95 (d, J = 20.0 Hz, 1P).

Synthesis of [1′-^{3}H]-F$_2$CDP and [1′-^{3}H]-F$_2$CDP. [1′-^{2}H]-F$_2$C (90% 1′-^{2}H and a 60:40 mixture of α:β anomers) and [1′-^{3}H]-F$_2$C (SA 8700 cpm/nmol) were converted to the monophosphate and then diphosphate as described above.

Covalent Modification of wt-RNR and C225S-RNR with [1′-^{3}H]-F$_2$CDP or [5-^{3}H]-F$_2$CDP. The reaction mixture contained the following in a final volume of 210 μL: 3 μM α2 (wt or mutant), 3 μM β2 (wt or 6 × His), 6 or 15 μM [5-^{3}H]-F$_2$CDP or [1′-^{3}H]-F$_2$CDP, 1.6 mM ATP, buffer A, and no reductant or reductant (either 5 mM DTT or 20 μM TR, 0.5 μM TRR, and 1.0 mM NADPH).

All reaction components except for F$_2$CDP were mixed and equilibrated at 25 °C for 5 min. A 5 μL aliquot of the reaction mixture was removed prior to inhibitor addition and at the end of 20 min and assayed for activity. Two hundred microliters was then loaded directly onto a Sephadex G-50 column (1 × 25.5 cm) equilibrated in 50 mM HEPES, pH 7.6. Fractions of 1 mL were collected. Aliquots of each fraction (500 μL) were assayed by scintillation counting, and the protein was quantitated by A_{280nm}.

Quantitation of Cytosine Released during the Inactivation of E. coli RNR by [5-^{3}H]-F$_2$CDP. The reaction mixture contained the following in 750 μL: 3 μM α2 and β2 and 6 μM [5-^{3}H]-F$_2$CDP (6643 cpm/nmol, 2 equiv/α2), 1.6 mM ATP, and 20 μM TR, 0.5 μM TRR, 1.0 mM NADPH in 50 mM HEPES, pH 7.6, 15 mM MgSO$_4$, and 1 mM EDTA. The reaction was incubated for 20 min at 25 °C. The mixture was then filtered through an YM-30 Centricon device (Millipore) at 4 °C. F$_2$C (80 nmol) and cytosine (120 nmol) were added as carriers before filtration. The flow-through was treated with 30 units of alkaline phosphatase (Roche) for 2 h at 37 °C and filtered through a second YM-30 Centricon device. The flow-through was analyzed

using a Waters 2480 HPLC with an Altech Adsorbosphere nucleotide nucleoside C-18 column (250 mm × 4.6 mm) at a flow rate of 1 mL/min. The elution buffer contained the following: buffer I, 10 mM NH$_4$OAc, pH 6.8; buffer II, 100% methanol. A 10 min isocratic elution with buffer I was followed by a linear gradient to 40% buffer II over 30 min. A linear gradient was then run to 100% buffer II over 5 min. Fractions (1 mL) were collected, and 200 μL of each was analyzed by scintillation counting. The recovery of [5-^{3}H]-cytosine and [5-^{3}H]-F$_2$C was calculated based on the UV spectrum (cytosine, λ_{267nm}, ε = 6100 M^{-1} cm^{-1}; F$_2$C, λ_{268nm}, ε = 9360 M^{-1} cm^{-1}) and normalized for carrier added. The radioactivity recovered with [5-^{3}H]-cytosine and [5-^{3}H]-F$_2$C was analyzed by scintillation counting.

Inactivation of RNR with F$_2$CDP Monitored by 140 GHz EPR Spectroscopy. A final volume of 15 μL contained 1.6 mM ATP, 75 μM wt-α2, 75 μM β2, and 300 μM F$_2$CDP in buffer A at 25 °C. The reaction was initiated by the addition of F$_2$CDP, and aliquots were drawn into Suprasil capillaries (silica, o.d. 0.55 mm, i.d. 0.4 mm, from Wilmad LabGlass) by capillary action. The samples were frozen in liquid N$_2$ at 30 s to 3 min after initiation.

Spectra were acquired at 60 K on a custom-designed pulsed spectrometer (*33*). Echo-detected spectra were acquired using a stimulated echo sequence with a pulse length of $t_{\pi/2}$ = 72 ns and a pulse spacing of τ = 230 ns or a pulse length of $t_{\pi/2}$ = 65 ns and a pulse spacing of τ = 200 ns. As previously demonstrated, the time domain approach allowed us to filter out the new radical from the Y· (*34*). The external magnetic field was swept with the assistance of a field lock described previously (*34*). The echo intensity at each field position was integrated, and an average of 1000 samples per point was taken.

9 GHz EPR Experiments and Simulations of the Reaction of RNR and C225S-RNR with [1′-^{x}H]-F$_2$CDP (x = 1 or 2). All reactions were carried out in a final volume of 230 μL and contained 15 μM α2, 15 μM β2, 75 μM F$_2$CDP, and 1.6 mM ATP in buffer A at 25 °C. The reaction was initiated by the addition of F$_2$CDP, and at 45 s, the reaction mixture was transferred into a calibrated 706 PQ EPR tube (Wilmad) and frozen in liquid N$_2$. EPR spectra were acquired on a Bruker ESP-300 spectrometer at 77 K. Spectra were acquired at 20 μW with 100 kHz modulation frequency, 1 G modulation amplitude, conversion time of 20.48 ms, and time constant of 5.12 ms. Typically, the sweep width was 150 G, and 2048 points were acquired per spectrum. Simulations of the 9 GHz EPR spectra were performed with either SimFonia or EasySpin (*35*). The g-values determined from the 140 GHz spectra were g_x = 2.00738, g_y = 2.00592, and g_z = 2.00230. All spectra were simulated with a Lorentzian to Gaussian line shape broadening ratio of 1. Parameters for the line width and the components of the hyperfine coupling tensor, A_{xx}, A_{yy}, and A_{zz}, were varied to obtain the best fit.

Analysis of the Reaction of wt- and C225S-RNR with F$_2$CDP by SDS-PAGE. The inactivation mixture contained in a final volume of 50 μL 5 μM α2 and β2, 3 mM ATP, with or without 5 mM DTT, and buffer A. The reaction was initiated by addition of 2.5 equiv of F$_2$CDP (12.5 μM) and incubated at 25 °C for 5 min. The inactivation mixture (8 μL) was mixed with 8 μL of 2× loading buffer ± β-ME. The samples were either heated at 90 °C for 2 min or not heated before loading on a 10% SDS-PAGE gel. The proteins were visualized with Coomassie blue staining. The band intensities were quantified using Quantity One software from Bio-Rad.

RESULTS

Time-Dependent Inactivation of RNR or C225S-RNR by F_2CDP. The assay for activity of *E. coli* RNR is unusual in that the two subunits have weak affinity for one another that is dependent on the presence of nucleotides. The K_d for subunit interaction with CDP/ATP is 0.2 μM (*36*). Typically, the activity of each subunit is assayed independently by adding a large excess of the second subunit. A second complexity of the assay is that activity is not directly proportional to the concentration of enzyme. At higher enzyme concentrations, for example, the rates of the reactions are typically slower (*26*). These complexities are likely associated with the coupled assay that requires rereduction of the disulfide bond accompanying nucleotide reduction by TR/TRR/NADPH.

Time-dependent inactivation experiments of *E. coli* RNR by F_2CDP were initially carried out at 15 μM α2 and β2 using a 5-fold molar excess of F_2CDP. To examine the stoichiometry of inactivation under physiological concentrations of RNR, the time-dependent inactivation studies were reexamined with α2 and β2 at 3 μM and F_2CDP at 3 μM in the absence of reductant. The assay was monitored in two ways. In method 1, the inactivation mixture was diluted 10-fold and assayed for dCDP production directly. Under these conditions (Figure 1A) the enzyme was completely inactivated with one F_2CDP per α2. In method 2 the inactivation mixture was diluted 20-fold with a 5-fold excess of the subunit not being assayed. Under these conditions β2 lost 90% of its activity associated with loss of the Y$\cdot$ (Figure 1B, red), and α2 lost 40% of its activity with some activity recovered with time (Figure 1B, blue). These results are very similar to the previous studies carried out at 15 μM RNR (*15*, *18*) and also indicate that RNR is completely inactivated with one F_2CDP per α2β2.

Time-Dependent Inactivation of C225S-α2$\cdot$$\beta$2 by F_2CDP. In our earlier experiments, C754S/C759S-α2β2 in the presence of TR/TRR/NADPH behaved like the wt-RNR in the absence of reductant, as judged by time-dependent inactivation of β2 and by detection of the new radical by EPR methods (*15*). C754 and C759 are located in the C-terminal tail of α2 and are responsible for rereduction of the active site disulfide on each turnover (*21*). In the presence of DTT, a reductant that can rereduce the active site directly, inactivation of C754S/C759S-α2β2 proceeded as with wt-RNR in the presence of reductants, either TR/TRR/NADPH or DTT. These results together suggested that the mode of inactivation observed in the presence of reductants requires the delivery of reducing equivalents to the active site. This model further suggests that C225 and C462 may be oxidized during the inactivation process and that rereduction of the disulfide may be necessary for the alkylation mode. Given this hypothesis, time-dependent inactivation of both subunits of C225S-α2β2 by F_2CDP (method 2, above) was monitored in the absence of reductant and in the presence of TR/TRR/NADPH or DTT. The results of activity assays for β2 under these conditions are shown in Figure 1C. Under all conditions, C225S-α2β2 exhibits a pattern of β2 inactivation that is characteristic of the wt-RNR in the absence of reductants (compare Figure 1C with Figure 1B, red).

C225S-α2β2 with [$1'$-^{3}H]-F_2CDP: Sephadex Chromatography To Monitor Covalent Labeling. If C225 is essential for inactivation by the alkylative pathway, then incubation of [$1'$-^{3}H]-F_2CDP with C225S-α2β2 should result in greatly reduced labeling relative to wt-RNR (1 equiv of ^{3}H/α2) in the presence of reductant. When C225S-α2β2 was incubated with [$1'$-^{3}H]-
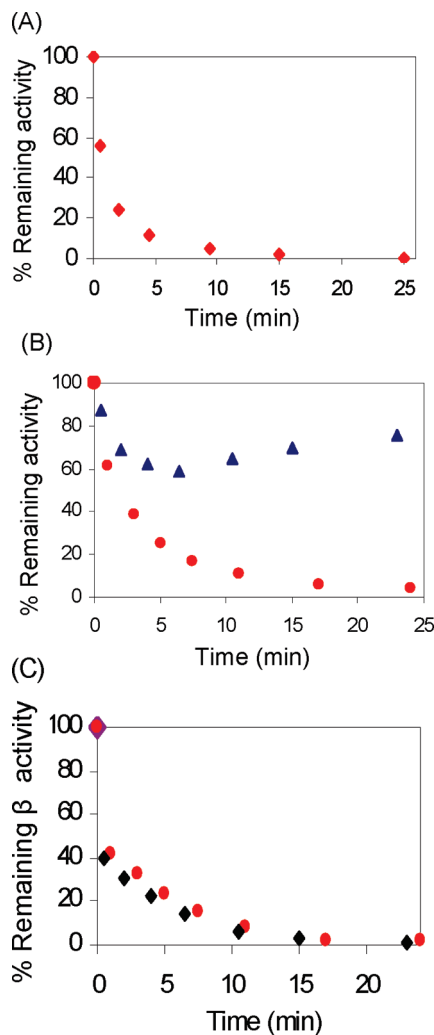

FIGURE 1: Time-dependent inactivation of *E. coli* wt-RNR (3 μM) or C225S-RNR by F_2CDP (3 or 6 μM) in the absence of reductant, assayed by method 1 or method 2. (A) Method 1: inactivation mixture diluted 10-fold with 1 F_2CDP/α2. (B) α (blue ▲) and β (red ●) inactivation mixture diluted 20-fold in the presence of a 5-fold excess of the second subunit. (C) Method 2: as in (B) except C225S-RNR replaced wt-RNR. The remaining β activity was assayed in the absence of reductant (red ●) and in the presence of reductant (DTT, black ◆).

F_2CDP in the presence of TR/TRR/NADPH and ATP, 0.14 equiv of the inhibitor was associated with the protein under native conditions (average of two runs) and 0.15 equiv was associated under denaturing conditions. These data support the proposal that C225 is required for the majority of labeling that occurs in the wt reaction in the presence of reductants.

SDS-PAGE of RNR Inactivated by F_2CDP in the Presence and Absence of Reductant. Our recent studies on *L. leichmannii* RNR and human RNRs indicated that SDS-PAGE analysis of the enzyme subsequent to its inactivation by F_2CTP (*L. leichmannii*) and F_2CDP (human) resulted in 35−50% of α migrating more slowly on the gel relative to the wt-α (*24*, *25*). This altered conformation of α appeared to be associated with the extent of covalent labeling by the sugar moiety from the inhibitor. A similar analysis was carried out on the *E. coli* RNR/F_2CDP reaction mixture in the presence and absence of reductant (Figure 2). Lanes 1−4 contain the inactivation mixture in the presence of the reductant DTT, and lanes 5−8 are identical to lanes 1−4 without DTT. Lane 1 is the reaction
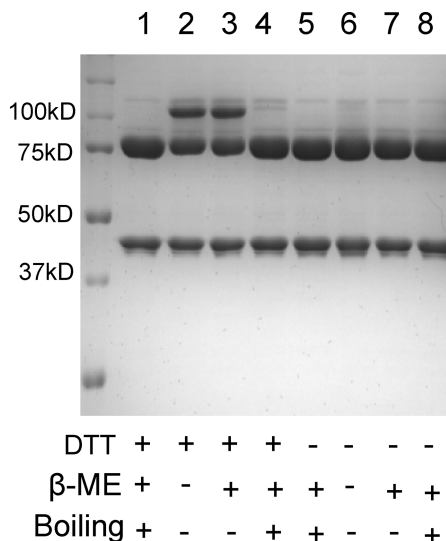
FIGURE 2: SDS-PAGE (10%) analysis of the α/β complex (5 μM) inactivated by F$_2$CDP (12.5 μM) and ATP (3 mM) in the presence or in the absence of DTT at 25 °C for 5 min. Each sample was mixed with 2× loading buffer ± β-ME ± boiling for 2 min before loading as indicated. A band at 110 kDa is observed in lanes 2 and 3 (inactivation in the presence of DTT, without boiling).

mixture prior to addition of F$_2$CDP, and lane 4 shows the results when the sample is boiled prior to loading the gel. A slowly migrating band is observed in the presence of DTT and when the sample is loaded without boiling (lanes 2 and 3, Figure 2). Appearance of this new band is associated with loss of α. We propose that this new species is an altered conformation of α that migrates like a protein of 110 kDa. Several pieces of evidence support this proposal. First, our recent mutagenesis studies with the human RNRs suggested that C218 (equivalent to C225 in the *E. coli* RNR) plays an important role in covalent modification of the enzyme (*37*). When C218S-hRNR and β or β′ were inactivated by F$_2$CDP/ATP altered migration of α occurred in the presence or absence of DTT. Furthermore, boiling of the sample resulted in loss of its altered migratory properties as with *E. coli* RNR (*37*). Second, preliminary mass spectrometric analysis of a tryptic digest of this species with altered migratory properties reveals that it is α (data not shown). Third, the adenosylcobalamin-dependent class II RNR that is a monomer homologous to α shows altered migratory properties (*24, 25*).

Cytosine Production Accompanies Inactivation: Use of [5-³H]-F$_2$CDP. Our previous studies with *E. coli* RNR (15 μM) and F$_2$CDP and more recent studies with hRNR (5 μM) and [5-³H]-F$_2$CDP both indicated that 0.5 equiv of cytosine/α is produced during the inactivation (*15, 18*). In this study, the experiments were repeated with *E. coli* RNR (3 μM). In the presence and absence of DTT, the amount of cytosine released was determined by HPLC, and the amount retained with the protein was determined by Sephadex G50 chromatography. In the presence of DTT, the amount of cytosine released after a 20 min incubation was 0.85 equiv/α, and the amount of ³H associated with the protein was 0.08 equiv (average of three experiments). The remaining radioactivity was recovered as F$_2$C, subsequent to phosphate removal and accounted for mass balance. The amount of cytosine released is greater than previously reported from studies with higher enzyme concentrations (15−75 μM), although quantitation was more difficult as labeled F$_2$CDP was not available. Thus with 3 μM RNR and DTT, between 0.5 and 1 F$_2$CDP/α is required for complete inactivation.
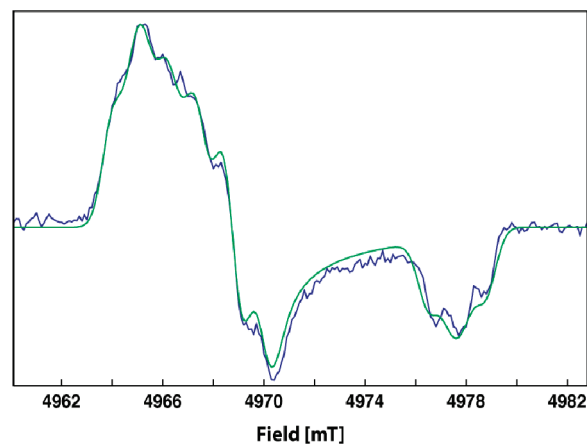

FIGURE 3: Echo-detected 139.5 GHz EPR spectrum of F$_2$CDP-inactivated RNR recorded at 65 K. 1000 shots were accumulated for each point in the spectrum. The stimulated echo pulse width was $t_{\pi/2}$ = 56 ns and t_p = 200 ns. g-values obtained from the spectrum are as follows: g_x = 2.00738, g_y = 2.00592, and g_z = 2.00230. Two hyperfine couplings were used in the simulation with A_1 = (11.4, 14.6, 12.8) and A_2 = (8.5, 8.5, 8.5).

In reactions carried out without DTT, the amount of cytosine determined varied from 0.1 to 0.15 equiv/α (from 12 experiments) after a 20 min incubation, after the inactivation was complete. Analysis of radiolabel associated with the protein by Sephadex G50 chromatography gave 0.075 equiv/α and when the chromatography was carried out with ATP in the eluent, 0.125 equiv/α. When the same experiment was carried out after a 5 min incubation and the Sephadex chromatographic analysis was shortened to 12 min, only 0.08 equiv/α was still associated with the protein. The small amounts of cytosine recovered with the protein in these experiments will be discussed subsequently. In contrast to the experiments carried out in the presence of reductant, the remainder of the radioactivity, subsequent to dephosphorylation, migrated on a reverse-phase HPLC column as a broad peak with retention times similar to nucleoside analogues of cytidine. Analysis of these products would likely require their stabilization by NaBH$_4$ reduction as successfully carried out with *L. leichmannii* RNR inactivated by F$_2$CTP (*24, 25*).

Structure of the New Radical at 140 GHz. In our previous studies of inactivation of RNR by F$_2$CDP in the absence of reductant, a new radical was generated concomitant with loss of the Y·. Forty percent of the Y· was lost on a rapid (30 s) time scale at 75 μM RNR. The analysis of the new radical was challenging at 9 GHz due to the spectral overlap between the new radical and the Y·. Our previous studies have demonstrated that high-field pulsed EPR at 140 GHz can be used to facilitate deconvolution of overlapping spectra (*34*). This method takes advantage of fact that the Y· is adjacent to a diferric cluster and thus its signal has an enhanced spin-lattice relaxation time relative to that expected for the new radical which is located in α > 35 Å from the Y·. Thus analysis of the spectrum of the inactivation mixture at 60 K by this method gave the first clear view of the new radical (Figure 3) and allowed determination of its g-values (2.00738, 2.00592, 2.0023). The high-field spectrum and the g-values of the new radical are strikingly similar to those obtained of a radical derived from CDP when E441Q-α was incubated with TTP, DTT, and β (*23*). Extensive ENDOR, EPR, and computational studies in conjunction with isotopic labeling studies using [1′-²H]- and [4′-²H]-CDP revealed the structure of this radical to be semidione nucleotide radical (**4**, Figure 4). Thus
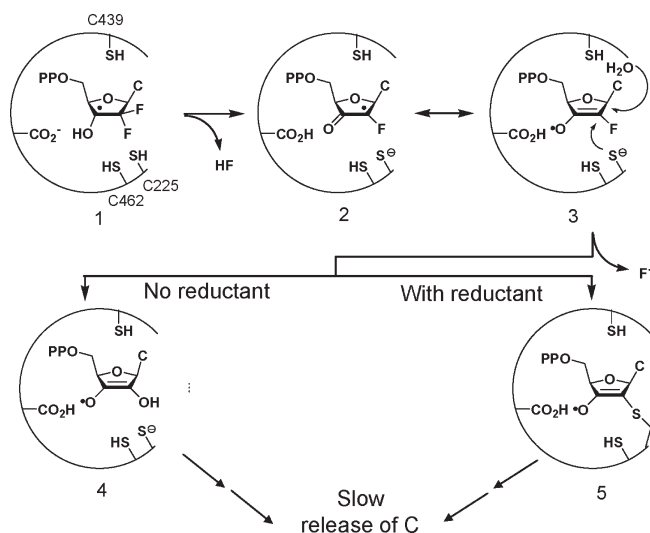
FIGURE 4: Proposed mechanism of inactivation of RNR by F_2CDP in the absence (**4**) and the presence (**5**) of reductant.

we propose that the structure of the new radical observed during the F_2CDP inactivation with no reductants is **4**.

EPR Spectrum at 9 GHz of wt-RNR Inactivated with [1′-²H]-F₂CDP. To obtain evidence in support of **4** (Figure 4) as the structure of the new radical, wt-RNR (15 μM) was incubated for 45 s with [1′-¹H]-F_2CDP/ATP, and the sample was frozen in liquid N_2 and examined by 9 GHz EPR spectroscopy (Figure 5A, red). Subtraction of the Y· (Figure 5A, blue) from this spectrum gave the spectrum of the new radical (black). This spectrum is very similar to that we previously reported with 75 μM RNR (*15*). Under these conditions, within 45 s, 50−60% of the Y· was lost and 0.4−0.48 equiv of the new radical was observed. These values are higher than those previously reported due to the higher RNR concentrations used and the slower rates of inactivation in the previous studies. We have previously observed with mechanism-based inhibitors that higher concentrations of RNR used to obtain EPR spectra result in slower inactivation rates. The basis for the kinetic differences are not understood but may be related to altered quaternary structure.

An identical experiment was then carried out with [1′-²H]-F_2CDP with the results shown in Figure 5B. Subtraction of Y· (blue) resulted in the spectrum in black in which the apparent triplet (Figure 5A) has collapsed to a doublet. A similar experiment using [U-²H]-β2 gave a spectrum similar to that in Figure 5A (data not shown). The amount of new radical formed was 80% that of the Y· lost, which suggests that 0.4 equiv/α was generated. If **4** is indeed the structure of the new radical (Figure 4), then cytosine should be retained by the protein in an amount equivalent to the amount of new radical. The cytosine comigrating with protein, however, is lower (0.08) than expected based on the 0.25 vs 0.4 equiv of radical. It becomes closer (0.125 equiv) when the protein was chromatographed with ATP effector in the elution buffer. We will argue subsequently that this discrepancy is associated with the analytical method for cytosine recovery, and hence we still favor the structure of **4** in Figure 4 for the new radical.

EPR Spectrum at 9 GHz of C225S-RNR Inactivated with [1′-²H]-F₂CDP. C225S-α2β2 was incubated with [1′-¹H]-F_2CDP/ATP in the absence or presence of reductants (TR/TRR/NADPH or DTT). The time-dependent inactivation studies (Figure 1C) indicate that under all conditions a new radical identical to that in Figure 5A should be observed.
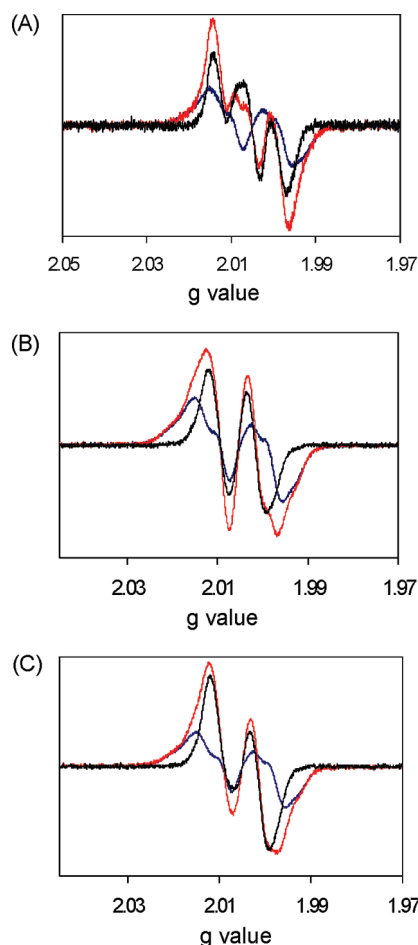

FIGURE 5: EPR spectrum at 9 GHz of *E. coli* wt-RNR (15 μM) or C225S-RNR (15 μM) inactivated by F_2CDP or [1′-²H]-F_2CDP. (A) The reaction mixture with F_2CDP was frozen in liquid N_2 at 45 s (red) and is a composite of Y· and new radical. The Y· (blue) was subtracted from the red spectrum to give the black spectrum of the new radical. (B) As in (A) except that [1′-²H]-F_2CDP replaced F_2CDP. (C) As in (A) except that C225S-RNR and [1′-²H]-F_2CDP replaced wt-RNR and F_2CDP.

Furthermore, with [1′-²H]-F_2CDP, a collapse in the hyperfine structure would be expected. In the former case a triplet spectrum very similar to that shown in Figure 5A was in fact observed (data not shown), and the results of the latter experiment are shown in Figure 5C. The serine mutant of C225 still allows the chemistry to occur to generate the new radical.

DISCUSSION

Phosphorylated gemcitabine is a stoichiometric mechanism-based inhibitor of class I and II ribonucleotide reductases (*15*, *17*). Despite the stoichiometry, however, the mechanism(s) of inactivation revealed by the current studies and our previous studies is (are) very complex and involve(s) multiple pathways. We have recently shown, for example, that with the class I RNRs, both the *E. coli* and human enzymes, inactivation with [1′-³H]-F_2CDP in the presence of reductants results in 0.5 label/α and that it is due to increased affinity of the two subunits for one another relative to their affinity observed in the presence of the normal substrate/effector pairs (*18*).

Our past and current studies on *E. coli* and *L. leichmannii* RNRs have led to a model to account for the pathway of inactivation in the absence of reductant in which Y· is lost and a new, nucleotide-based radical is generated. Our working model

is shown in Figure 4. In this model, the first step is 3′-hydrogen atom abstraction followed by loss of F⁻ (**1** to **3**, Figure 4). These steps are analogous to those suggested for the reaction of RNR with 2′-fluoro-2′-deoxynucleoside 5′-diphosphate where we showed that the enzyme catalyzes partitioning between inactivation through a 3′-ketodeoxynucleotide and ultimately furanone formation and deoxynucleotide formation based. The partitioning depended on the presence of reductant and differed with TR/TRR/NADPH and DTT (*11*, *38*). The next step in the model is that water attacks the 2′ carbon to generate **4** concomitant with loss of the second F⁻. Intermediate **4** is proposed to be the new nucleotide radical detected by EPR spectroscopy. The conversion of **3** to **4**, to our knowledge, has no chemical precedent. This step is the reverse of water loss in the normal reduction process and requires that there is a water in the active site in the vicinity of the C2′ carbon. A similar mechanism for covalent modification of RNR by C225 (**5**, Figure 4) has been proposed by Ramos and co-workers based on DFT calculations (*19*) and previously by us (**5**, Figure 5). Unfortunately, the charges on the intermediate proposed in the Ramos model (12 in their Scheme 2) appear to be incorrect. Thus the kinetic "feasibility of nucleophilic attack at C2′ and its dependence on the nucleophile" needs to be reexamined computationally. In our proposed mechanism (Figure 4), we have ignored the fate of the fluorides and the source of water. Our biochemical studies, however, have shown that both fluorides are lost, at different rates, and an X-ray structure of the *Saccharomyces cerevisiae* α with F₂CDP and AMPNP (a nonhydrolyzable analogue of ATP) soaked into the active site suggests that waters are present on the bottom face of the nucleotide (*39*). The *S. cerevisiae* structure, if applicable to the *E. coli* RNR, also suggests that covalent modification of the sugar moiety derived from F₂CDP would likely be by C225. This cysteine and water are the only nucleophiles close to the sugar in the structure. E441, known to be essential for catalysis and located on the bottom face of the nucleotide, is displaced from its interaction with the 3′-OH of the nucleotide and thus is unlikely to be involved in covalent modification. Finally, as with all mechanism-based inhibitors (*10*), cytosine is eventually lost. This loss is usually associated with transformation of some intermediate (**4** or **5**, Figure 4) into a 3′-ketone that then slowly loses cytosine.

Several pieces of data from the present studies support the model in Figure 4. The first is that the new radical is nucleotide-based as it exhibits hyperfine interaction with the C-1′ proton consistent with **4**. The proposal of **4** as the new radical is also supported by our recent investigations of the mechanism by which E441Q-α in the presence of CDP, allosteric effector TTP, and β2 results in Y· loss and formation of a new nucleotide radical derived from CDP (*23*). Extensive isotope labeling experiments (including [4′-²H]- and [1′-²H]-CDP) in conjunction with ENDOR and EPR spectroscopy and computational analysis provided strong evidence that **4** is the structure generated. It should be noted, however, that the mechanism by which **4** is generated is not understood in either case and when derived from CDP and E441Q-α must be distinct from when it derived from F₂CDP and α. In addition, recent studies on the inactivation of the *L. leichmannii* RNR by F₂CTP resulted in trapping of a cytidine analogue thought to be derived from oxidation of radical **4** during NaBH₄ trapping (*24*). Finally, a monofluorinated cytidine derivative (**3**, Figure 4) was also trapped with NaBH₄ with the C119S mutant (C225 equivalent in the *L. leichmannii* RNR) (*24*, *25*, *38*).

The mechanism (Figure 4) predicts that the new radical still has its cytosine moiety attached. Thus experiments with [5-³H]-F₂CDP and isolation of RNR should reveal if the stoichiometry of the radical is equivalent to the amount of base residing with the protein. The analysis, however, is complicated for several reasons. First, the amount of the new radical is difficult to quantitate due to its spectral overlap with the Y·. Second, both radicals decay with time. Third, most experiments to look for cytosine release were all carried out subsequent to a 20 min incubation, while the new radical is formed within 45 s. The complete inactivation occurs over 20 min in which case the new radical is likely decomposing with loss of cytosine. Thus the observed value of 0.08−0.12 ³H/α and the estimation of 0.4 new radical/α, given the complications, suggest that base can still be attached to the new radical, consistent with **4**.

Finally, the studies with the C225S mutant support the proposed mechanism of inactivation in that no redox chemistry is involved in formation of the new radical and thus no reducing equivalents are required for inactivation involving loss of Y·. Furthermore, the studies with this mutant support the importance of C225 in the alkylative pathway (**5**), the one involving covalent modification of the protein. With the mutant, no label is attached to the protein despite the fact that this mutant can catalyze the first few steps in the pathway.

Our efforts to isolate and identify a peptide(s) labeled in the alkylative pathway have revealed that the alkylated product can rearrange during the workup. Even efforts to trap the alkylated adduct(s), likely a ketone moiety or an α,β-unsaturated ketone, by reduction with NaBH₄, which should preclude rearrangements, have been unsuccessful. Similar studies on the hRNR have also been unsuccessful. Only in the case of the *L. leichmannii* RNR has a peptide, containing the C-terminal cysteines attached to a sugar derived from F₂CTP, been identified (*24*). Even in that case, however, the recovery of total label in that peptide relative to total label attached to the protein is low, indicating that other nonisolable adducts are also generated. Our inability to identify a site(s) of labeling is unusual given that the inactivation is stoichiometric. The difficulty is likely related to reorganization of furanone-like moieties, by reverse Michael additions, prior to trapping with reductant (*11*). The observation that C225S-α is labeled at 10% that of the wt-α supports the role of C225 in alkylation, perhaps via cross-linking with a cysteine in the C-terminal tail of α. Finally, the unusual observation made with all RNRs examined thus far is that, accompanying their inactivation, an altered conformation of the α subunit is generated which migrates as 110 kDa protein by SDS-PAGE (Figure 2). Recent crystallization of the complex of the *E. coli* RNR inactivated by F₂CDP and analysis of the crystals by SDS-PAGE indicate the presence of this altered α structure (Stock and Drennan, unpublished results). We propose that C225 and a C-terminal cysteine are both bound to the sugar derived from F₂CDP during inactivation, causing a substantial change in the structure of α.

In the past few years we have examined in some detail the mechanisms by which the hRNR (both β′ and β) and *L. leichmannii* RNR are inactivated by F₂CDP or F₂CTP (*18*, *37*). They share many striking similarities despite the difference in cofactor requirement and quaternary structures. In all cases, despite stoichiometric inactivation, multiple pathways are required to account for the observed results. The mechanism by which F₂CDP inactivates RNR *in vivo* remains to be unraveled. However, it is likely that the alkylative pathway is the mechanism involved given the availability of reductants. The tight complex

formed between the two subunits of the class I RNRs after incubation with F$_2$CDP and our ability to radiolabel the sugar moiety of F$_2$CDP that ends up covalently bound to the protein may allow us to assess if similar chemistry is occurring inside the cell.

ACKNOWLEDGMENT

REFERENCES

1. Hertel, L. W., Boder, G. B., Kroin, J. S., Rinzel, S. M., Poore, G. A., Todd, G. C., and Grindey, G. B. (1990) Evaluation of the antitumoractivity of gemcitabine (2′,2′-difluoro-2′-deoxycytidine). *Cancer Res. 50*, 4417–4422.

2. Huang, P., Chubb, S., Hertel, L. W., Grindey, G. B., and Plunkett, W. (1991) Action of 2′,2′-difluorodeoxycytidine on DNA-synthesis. *Cancer Res. 51*, 6110–6117.

3. Plunkett, W., Huang, P., and Gandhi, V. (1997) Gemcitabine: actions and interactions. *Nucleosides Nucleotides 16*, 1261–1270.

4. Davidson, J. D., Ma, L., Flagella, M., Geeganage, S., Gelbert, L. M., and Slapak, C. A. (2004) An increase in the expression of ribonucleotide reductase large subunit 1 is associated with gemcitabine resistance in non-small cell lung cancer cell lines. *Cancer Res. 64*, 3761–3766.

5. Duxbury, M., Ito, H., Zinner, M. J., Ashley, S. W., and Whang, E. E. (2004) RNA interference targeting the M2 subunit of ribonucleotide reductase enhances pancreatic adenocarcinoma chemosensitivity to gemcitabine. *Oncogene 23*, 1539–1548.

6. Arner, E. S., and Eriksson, S. (1995) Mammalian deoxyribonuclease kinases. *Pharmacol. Ther. 67*, 155–186.

7. Hsu, S. H., Liou, J. Y., Dutschman, G. E., and Cheng, Y. C. (2005) Phosphorylation of cytidine, deoxycytidine, and their analog monophosphates by human UMP/CMP kinase is differentially regulated by ATP and magnesium. *Mol. Pharmacol. 67*, 806–814.

8. Van Rompay, A. R., Johansson, M., and Karlsson, A. (1999) Phosphorylation of deoxycytidine analog monophosphates by UMP-CMP kinase: molecular characterization of the human enzyme. *Mol. Pharmacol. 56*, 562–569.

9. Cheng, Y. C., Agarwal, R. P., and Parks, R. E., Jr. (1971) Erythrocytic nucleoside diphosphokinase. IV. Evidence for electrophoretic heterogeneity. *Biochemistry 10*, 2139–2143.

10. Stubbe, J., and van der Donk, W. A. (1995) Ribonucleotide reductases: radical enzymes with suicidal tendencies. *Chem. Biol. 12*, 793–801.

11. Stubbe, J., and van der Donk, W. A. (1998) Protein radicals in enzyme catalysis. *Chem. Rev. 98*, 705–762.

12. Gandhi, V., and Plunkett, W. (1990) Modulatory activity of 2′,2′-difluorodeoxycytidine on the phosphorylation and cytotoxicity of arabinosyl nucleosides. *Cancer Res. 50*, 3675–3680.

13. Heinemann, V., Xu, Y. Z., Chubb, S., Sen, A., Hertel, L. W., Grindey, G. B., and Plunkett, W. (1990) Inhibition of ribonucleotide reduction in Ccrf-Cem cells by 2′,2′-difluorodeoxycytidine. *Mol. Pharmacol. 38*, 567–572.

14. Gandhi, V., Huang, P., Xu, Y. Z., Heinemann, V., and Plunkett, W. (1991) Metabolism and action of 2′,2′-difluorodeoxycytidine: self-potentiation of cytotoxicity. *Adv. Exp. Med. Biol. 309A*, 125–130.

15. van der Donk, W. A., Yu, G. X., Perez, L., Sanchez, R. J., Stubbe, J., Samano, V., and Robins, M. J. (1998) Detection of a new substrate-derived radical during inactivation of ribonucleotide reductase from *Escherichia coli* by gemcitabine 5′-diphosphate. *Biochemistry 37*, 6419–6426.

16. Baker, C. H., Banzon, J., Bollinger, J. M., Stubbe, J., Samano, V., Robins, M. J., Lippert, B., Jarvi, E., and Resvick, R. (1991) 2′-deoxy-2′-methylenecytidine and 2′-deoxy-2′,2′-difluorocytidine 5′-diphosphates: potent mechanism-based inhibitors of ribonucleotide reductase. *J. Med. Chem. 34*, 1879–1884.

17. Silva, D. J., Stubbe, J., Samano, V., and Robins, M. J. (1998) Gemcitabine 5′-triphosphate is a stoichiometric mechanism-based inhibitor of *Lactobacillus leichmannii* ribonucleoside triphosphate reductase: evidence for thiyl radical-mediated nucleotide radical formation. *Biochemistry 37*, 5528–5535.

18. Wang, J., Lohman, G. J., and Stubbe, J. (2007) Enhanced subunit interactions with gemcitabine-5′-diphosphate inhibit ribonucleotide reductases. *Proc. Natl. Acad. Sci. U.S.A. 104*, 14324–14329.

19. Cerqueira, N. M., Fernandes, P. A., and Ramos, M. J. (2007) Understanding ribonucleotide reductase inactivation by gemcitabine. *Chem.—Eur. J. 13*, 8507–8515.

20. Pereira, S., Fernandes, P. A., and Ramos, M. J. (2004) Mechanism for ribonucleotide reductase inactivation by the anticancer drug gemcitabine. *J. Comput. Chem. 2004*, 1286–1294.

21. Mao, S. S., Holler, T. P., Yu, G. X., Bollinger, J. M., Booker, S., Johnston, M. I., and Stubbe, J. (1992) A model for the role of multiple cysteine residues involved in ribonucleotide reduction—amazing and still confusing. *Biochemistry 31*, 9733–9743.

22. Mao, S. S., Holler, T. P., Bollinger, J. M., Jr., Yu, G. X., Johnston, M. I., and Stubbe, J. (1992) Interaction of C225SR1 mutant subunit of ribonucleotide reductase with R2 and nucleoside diphosphates: tales of a suicidal enzyme. *Biochemistry 31*, 9744–9751.

23. Zipse, H., Artin, E., Wnuk, S., Lohman, G. J., Martino, D., Griffin, R. G., Kacprzak, S., Kaupp, M., Hoffman, B., Bennati, M., Stubbe, J., and Lees, N. (2009) Stucture of the nucleotide radical formed during reaction of CDP/TTP with the E441Q-α2β2 of *E. coli* ribonucleotide reductase. *J. Am. Chem. Soc. 131*, 200–211.

24. Lohman, G. J. S., and Stubbe, J. (2009) Inactivation of *Lactobacillus leichmannii* ribonucleotide reductase by F$_2$CTP: covalent modification (part I), Biochemistry (manuscript in preparation).

25. Lohman, G. J. S., Gerfen, G. J., and Stubbe, J. (2009) Inactivation of *L. leichmannii* ribonucleotide reductase by F$_2$CTP: adenosylcobalamin destruction and formation of a nucleotide based radical, Biochemistry (manuscript in preparation).

26. Ge, J., Yu, G. X., Ator, M. A., and Stubbe, J. (2003) Pre-steady-state and steady-state kinetic analysis of *E. coli* class I ribonucleotide reductase. *Biochemistry 42*, 10071–10083.

27. Yee, C. S., Seyedsayamdost, M. R., Chang, M.C. Y., Nocera, D. G., and Stubbe, J. (2003) Generation of the R2 subunit of ribonucleotide reductase by intein chemistry: insertion of 3-nitrotyrosine at residue 356 as a probe of the radical initiation process. *Biochemistry 42*, 14541–14552.

28. Bollinger, J. M. J., Tong, W. H., Ravi, N., Huynh, B. H., Edmondson, D. E., and Stubbe, J. A. (1995) Use of rapid kinetics methods to study the assembly of the diferric-tyrosyl radical cofactor of *E. coli* ribonucleotide reductase. *Methods Enzymol. 258*, 278–303.

29. Lunn, C. A., Kathju, S., Wallace, B. J., Kushner, S. R., and Pigiet, V. (1984) Amplification and purification of plasmid-encoded thioredoxin from *Escherichia coli* K12. *J. Biol. Chem. 259*, 469–474.

30. Russel, M., and Model, P. (1985) Direct cloning of the trxB gene that encodes thioredoxin reductase. *J. Bacteriol. 163*, 238–242.

31. Rylova, S. N., Albertioni, F., Flygh, G., and Eriksson, S. (2005) Activity profiles of deoxynucleoside kinases and 5′-nucleotidases in cultured adipocytes and myoblastic cells: insights into mitochondrial toxicity of nucleoside analogs. *Biochem. Pharmacol. 69*, 951–960.

32. Steeper, J. R., and Steuart, C. C. (1970) A rapid assay for CDP reductase activity in mammalian cell extracts. *Anal. Biochem. 34*, 123–130.

33. Bennati, M., Farrar, C. T., Bryant, J. A., Inati, S. J., Weis, V., Gerfen, G. J., Riggs-Gelasgo, P., Stubbe, J., and Griffin, R. G. (1999) Pulsed electron-nuclear double resonance (ENDOR) at 140 GHz. *J. Magn. Reson. 138*, 232–243.

34. Lawrence, C. C., Bennati, M., Obias, H. V., Barr, G., Griffin, R. G., and Stubbe, J. (1999) High-field EPR detection of a disulfide radical anion in the reduction of cytidine 5′-diphosphate by the E441Q R1 mutant of *Escherichia coli* ribonucleotide reductase. *Proc. Natl. Acad. Sci. U.S.A. 96*, 8979–8984.

35. Stoll, S., and Schweiger, A. (2006) A comprehensive software package for spectral simulation and analysis in EPR. *J. Magn. Reson. 178*, 42–55.

36. Climent, I., Sjöberg, B. M., and Huang, C. Y. (1992) Site-directed mutagenesis and deletion of the carboxyl terminus of *Escherichia coli* ribonucleotide reductase protein R2: effects on catalytic activity and subunit interaction. *Biochemistry 31*, 4801–4807.

37. Wang, J., Lohman, G. J., and Stubbe, J. (2009) Mechanism of inactivation of human ribonucleotide reductase with p53R2 by gemcitabine-5′-diphosphate, Biochemistry (DOI: 10.1021/bi901588z).

38. Stubbe, J., and Kozarich, J. W. (1980) Fluoride, pyrophosphate, and base release from 2′-deoxy-2′-fluoronucleoside 5′-diphosphates by ribonucleoside-diphosphate reductase. *J. Biol. Chem. 255*, 5511–5513.

39. Xu, H., Faber, C., Uchiki, T., Fairman, J. W., Racca, J., and Dealwis, C. (2006) Structures of eukaryotic ribonucleotide reductase I provide insights into dNTP regulation. *Proc. Natl. Acad. Sci. U.S.A. 103*, 4022–4027.